The impact of voltage independent carriers on implied voltage measurements on silicon devices

M. K. Juhl and T. Trupke
The School of Photovoltaics and Renewable Energy, The University of New South Wales, Sydney 2052, Australia

(Received 7 September 2016; accepted 6 October 2016; published online 25 October 2016)

The electrical performance a solar cell is determined from direct measurements of the current voltage relationship, while the so-called *implied* current-voltage measurements are often performed to estimate the performance of partially processed samples. Implied current voltage measurements are commonly obtained from quasi steady state photoconductance and quasi steady state photoluminescence measurements, where the implied voltage is inferred from the average excess carrier density. As will be shown here, this approach can be problematic due to the presence of excess carriers that *do not contribute* to the terminal voltage. These carriers are referred to as voltage independent carriers, a concept that is not widely known or generally accepted. This paper provides the theoretical background for the distinction of voltage dependent and voltage independent carriers. It is shown that the relative impact of voltage independent carriers on implied voltage data depends strongly on device parameters and on the illumination wavelength. Practical limits are provided for these parameters for which the voltage independent carriers can be neglected and for which an implied voltage thus accurately reflects the junction voltage. *Published by AIP Publishing.*
[http://dx.doi.org/10.1063/1.4965698]

I. INTRODUCTION

Implied current-voltage characteristics are measured under experimental conditions, where either the current, the voltage, or both are not directly measured at the terminals but rather inferred from other measurements. In Suns-V_{oc}[1,2] measurements the terminal voltage is measured, but the current is inferred from the absorbed photon flux under open circuit conditions. The latter approach is justified as the terminal current of a solar cell in the dark is equivalent to the total recombination rate in the device volume, and since the total generation rate (caused by illumination) equals the total recombination rate under open circuit-conditions. Going one step further, implied current-voltage data can also be obtained where both the current and the voltage are inferred. Techniques that provide such implied current-voltage data include photoconductance[2,3] or photoluminescence (PL)[4] measured simultaneously with the incident photon flux under variable illumination intensity.

The terminal voltage of a solar cell is determined by the splitting of the quasi-Fermi energies at the junction and thus by the excess minority carrier density at the junction. Photoconductance data however provides the *average* excess minority carrier density ($\Delta\bar{n}$) throughout the volume, and similarly the measured photoluminescence intensity is determined by the average separation of the quasi-Fermi energies. In both measurements, the presence of a carrier profile in the bulk that is independent of the junction voltage can cause problems in the interpretation of implied current-voltage data. This is the focus of this paper.

The need to distinguish voltage dependent carriers from voltage independent carriers first became apparent during the development of PL based series resistance imaging for silicon solar cells. The concept was born from the observation that when samples were illuminated and held under external short circuit conditions they still emitted luminescence.[5] In the classical interpretation, according to which the luminescence signal scales exponentially with the separation of the quasi Fermi energies, this observation did not make sense; the PL signal was expected to drop to zero. The discrepancy was attributed to photogenerated carriers that cannot diffuse to be collected at the junction. These carriers were therefore referred to as *diffusion limited carriers*. It was found that correct series resistance data could only be determined if the luminescence signal arising from the diffusion limited carriers was corrected for. The correction procedure involved subtracting a photoluminescence image measured under short circuit condition from photoluminescence images taken at any other bias condition.

The concept of diffusion limited carriers has also been used to correct the implied current-voltage measurements of shunted samples, acquired by the so-called Suns-PL measurement technique.[6] For shunted samples, the terminal voltage reduces sharply towards lower currents. This behaviour was confirmed in Suns-PL data down to a threshold voltage, below which the measured PL intensity was found to no longer be related to the terminal voltage, but rather scale linearly with illumination intensity. Abbott *et al*. confirmed this artefact in Suns-PL data to be caused by diffusion limited carriers and proposed a correction based on the subtraction of the PL signal from the diffusion limited carriers from the measured PL signal. Excellent agreement was found between the implied voltage and terminal measurements after this correction procedure.

However, in our view, the name *diffusion limited carriers* does not intuitively represent all situations in which excess carriers can be present within a device but do not

contribute to the terminal voltage. Consider two solar cells with different rear surface recombination velocities, held at short circuit conditions. Two such solar cells were simulated in PC1D V5.9[7] as 1 Ω cm, p-type, 180 μm thick, front junction devices. Both solar cells are illuminated with the AM1.5 g spectrum, and held at short circuit. The depth dependent excess carrier concentrations are shown in Figure 1 for rear surface recombination velocities of 0 cm/s (blue line) and 10^7 cm/s (orange line). The question can be asked if these two carrier distributions can both be considered to be diffusion limited, or whether they are rather limited by the cell's specific boundary conditions. The term "diffusion limited carriers" strictly only describes the carrier density for a sample with effectively infinite carrier sinks on both sides. In the example shown in Figure 1, this applies only to the solar cell with $S_r = 10^7$ cm/s. For this reason, we adopt the terminology of *voltage dependent carriers*, introduced earlier by Glatthaar *et al.*[8] This terminology also aligns with the work of Rau and Lan, who demonstrated that the photoluminescence intensity of a sample is described by a voltage dependent term and a voltage independent term.[9,10]

II. VOLTAGE INDEPENDENT CARRIERS

The concept of voltage dependent and voltage independent carriers may not be familiar to some readers, and even to many scientific experts in solar cell research. The presence of these carriers follows directly from the continuity equation for the quasi neutral region of a solar cell under monochromatic illumination being a inhomogeneous linear differential equation, as the generation rate is independent of the excess carrier density

$$\frac{d^2n[x]}{dx^2} = \frac{n[x]}{L^2} - \frac{\alpha N_\gamma e^{-\alpha x}}{D}, \tag{1}$$

where n is the minority carrier density, x is the distance from the front surface, L is the minority carrier diffusion length, D is the minority carrier diffusion constant, N_γ is the incident photon flux, and α is the absorption coefficient. The continuity equation presented here is strictly valid for a single pass of light through a sample, but the following analysis holds true for any broad-spectrum generation.

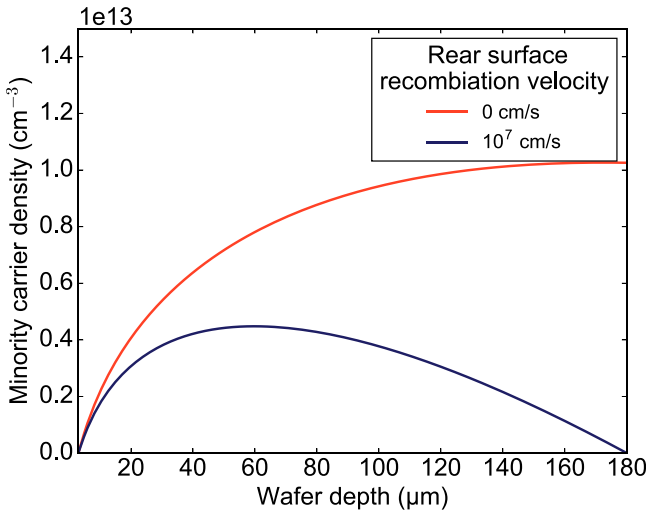

FIG. 1. PC1D simulations of two solar cells with different rear surface recombination velocities under external short circuit conditions.

As the continuity equation is a linear differential equation, it obeys the super position principle. For a homogeneous front junction device with a junction voltage (V) and with a rear surface recombination velocity (S_r), the following boundary conditions apply:

$$n[0] = n_0 e^{\frac{qV}{kT}}, \tag{2}$$

$$D\frac{dn}{dx}\bigg|_{x=W} = -S_r n[W], \tag{3}$$

where n_0 is the minority carriers density in the dark, q is the elementary charge, k is Boltzmann's constant, T is the temperature, and W is the thickness of the device.

The general solution to the continuity equation has the form

$$n = C_a e^{\frac{x}{L}} + C_b e^{-\frac{x}{L}} + C_c e^{-\alpha x}, \tag{4}$$

where C_a, C_b, and C_c are coefficients determined by the specific boundary conditions. Applying the boundary conditions in Equations (2) and (3), provide

$$C_a = -C_b - C_c + n_0 e^{\frac{qV}{kT}}, \tag{5}$$

$$C_b = \frac{1}{2D\cosh\left[\frac{W}{L}\right] + 2LS_r\sinh\left[\frac{W}{L}\right]}\Big(C_c\Big(LS_r\big(e^{-\alpha W} - e^{\frac{W}{L}}\big) - D\big(L\alpha e^{-\alpha W} + e^{\frac{W}{L}}\big)\Big) + n_0 e^{\frac{W}{L}} e^{\frac{qV}{kT}}(LS_r + D)\Big), \tag{6}$$

$$C_c = \frac{L^2 N_\gamma \alpha}{D\left(1 - (\alpha L)^2\right)}. \tag{7}$$

This solution can be re-arranged into voltage dependent (subscript vd) and voltage independent (subscript vid) terms

$$\Big(C_{a-vd}e^{\frac{qV}{kT}} + C_{a-vid}N_\gamma\Big)e^{\frac{x}{L}} + \Big(C_{b-vd}e^{\frac{qV}{kT}} + C_{b-vid}N_\gamma\Big)e^{\frac{-x}{L}} + C_{c-vid}N_\gamma e^{-\alpha x},$$

which can be written as

$$\big(C_{a-vd}e^{\frac{x}{L}} + C_{b-vd}e^{\frac{-x}{L}}\big)e^{\frac{qV}{kT}} + \Big(C_{a-vid}e^{\frac{x}{L}} + C_{b-vid}e^{\frac{-x}{L}} + C_{c-vid}e^{-\alpha x}\Big)N_\gamma, \tag{8}$$

or

$$n = n_{vd} + n_{vid}, \tag{9}$$

with

$$n_{vd} = \big(C_{a-vd}e^{\frac{x}{L}} + C_{b-vd}e^{\frac{-x}{L}}\big)e^{\frac{qV}{kT}}, \tag{10}$$

$$n_{vid} = \big(C_{a-vid}e^{\frac{x}{L}} + C_{b-vid}e^{\frac{-x}{L}} + C_{c-vid}e^{-\alpha x}\big)N_\gamma. \tag{11}$$

Note that the voltage independent terms are proportional to N_γ, whereas the voltage dependent carrier concentration

increases exponentially with the voltage. The presence of voltage and voltage independent carriers thus follows from the solution of the linear continuity equation. These carriers could equally be called illumination and illumination dependent carriers, however, the terminology voltage independent carriers is chosen as it is in terms of the terminal voltage, an important electrical output for solar cells.

In this paper, the discussion of the voltage dependent carriers is in the context of the junction voltage, which is equal to the terminal voltage only in the absence of resistive voltage drops. This occurs at open circuit conditions, the operating condition under which implied voltage measurements are normally performed.

In order to demonstrate the impact of voltage dependent and independent carriers, simulations were performed in PC1D (v5.92), of a solar cell that is dominated by front surface recombination and subjected to different monochromatic illumination wavelengths.

The simulated solar cell consists of a p-type wafer with the following parameters: thickness of 180 μm, resistivity 0.35 Ω cm, symmetric Shockley Read Hall carrier lifetimes of 100 μs for a mid gap defect,[11,12] front surface recombination velocity for electrons and holes of 1000 cm/s, and no rear surface recombination. The simulated device had a front phosphorous diffusion with an ERFC profile, a peak surface phosphorous concentration of 10^{19} cm^{-3}, and a junction depth of 0.4265 μm, resulting in a sheet resistance of ≈311.1 Ω/□. The illumination intensity was chosen for the bulk of the device to remain in low injection. The simulated solar cell also has an injection independent lifetime between open circuit and short circuit conditions. This allowed direct comparison between the carrier densities simulated under short circuit and under open circuit conditions.

The excess carrier densities at open circuit and at short circuit conditions were simulated for monochromatic illumination with wavelengths of 300, 750, 950, and 1100 nm. For each illumination wavelength, the illumination intensity was chosen to yield an open circuit voltage of 624.4 mV, which corresponded to illumination intensities of 10.00, 4.01, 3.46, and 46.85 mW/cm^2 for the respective illumination wavelengths.

The simulated minority carrier densities for open circuit conditions and short circuit conditions are shown in Figures 2(a) and 2(b). It is noted that the carrier densities at the junction (x = 0), shown in Figures 2(a) and 2(b), are identical in each case for the four illumination wavelengths, reflecting the fact that the terminal voltages are the same in each simulation. For comparison, the voltage dependent carrier density determined by simulating the device in the dark and under an applied bias of 624.4 mV is shown in Figure 2(a) as a black dotted line.

The simulated excess carrier profiles under illumination exceed the voltage dependent carrier distribution, except for the simulation with an illumination wavelength of 300 nm. For longer illumination wavelengths, the deviations between the total carrier densities and the voltage dependent carrier density profile become larger. Qualitatively this is expected as longer absorption depths result in more carriers being generated further away from the junction, which increases the concentration of voltage independent carriers. In contrast, for the 300 nm illumination, the incident photon flux is completely absorbed within the thin n-type region. The photogeneration profile then closely resembles the current injection at the junction under applied forward bias in the dark. Thus, no voltage independent carriers exist in the bulk and

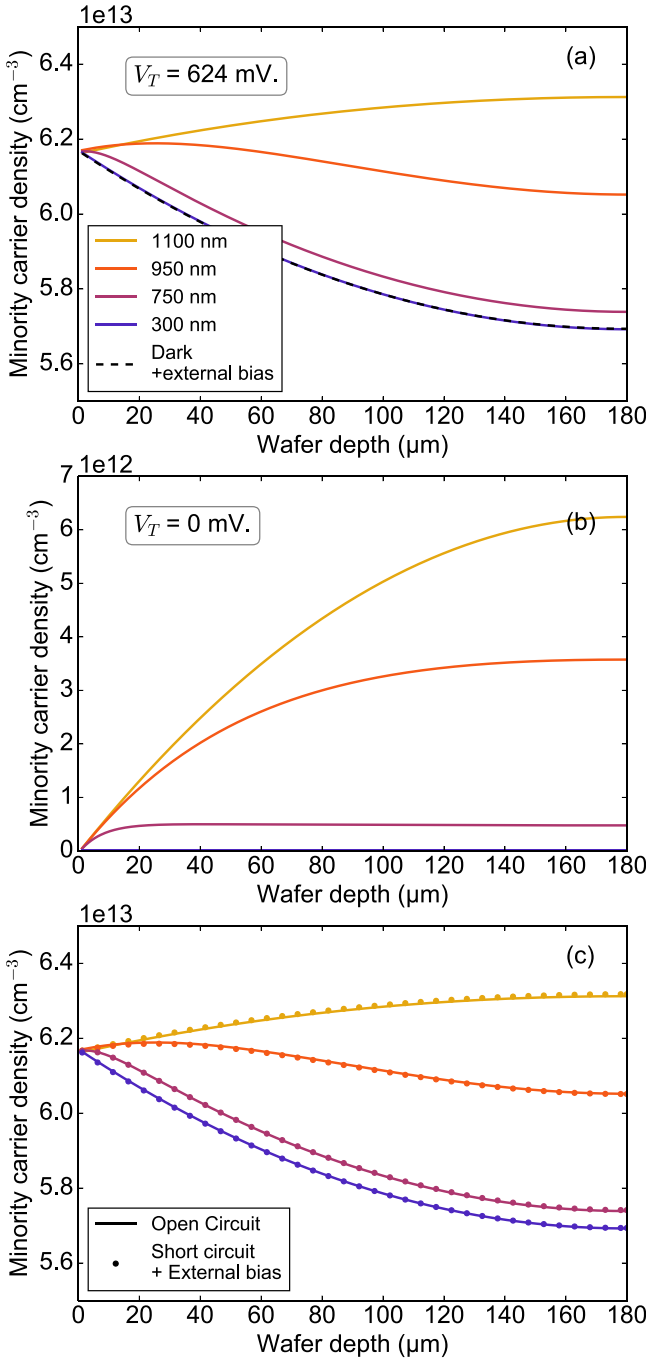

FIG. 2. (a) Simulated minority carrier profiles in the bulk of a front junction solar cell for different illumination wavelengths. The dashed lines represent the carrier density in the dark under forward bias of 624 mV, i.e., the voltage dependent carrier profile. For all wavelengths, the respective illumination intensities were chosen to result in 624 mV terminal voltage. (b) The same simulations but with the terminal voltage set to zero, represent the voltage independent carrier profiles. (c) Comparison of the carrier profiles under illumination at open circuit (lines) to the sum of the voltage dependent and voltage independent carrier profiles (symbols). Note, the "+" sign in the legend represents the mathematical addition of carrier density profiles.

the excess carrier profile under short wavelength illumination matches the voltage dependent carrier density profile.

For carriers to be truly voltage independent, they must maintain their location and magnitude as the voltage is changed. This is confirmed in Figure 2(c), with the comparison of the carrier concentration under illumination (the data from Figure 2(a)) to the sum of the voltage independent carrier density (the data from Figure 2(b)) and the voltage dependent carrier density (the dashed line in Figure 2(a)). The deviation between the carrier profiles for the same junction voltage in the dark and under illumination is thus exactly equal to the carrier profile at short circuit conditions for each illumination wavelength. This demonstrates that the carriers which do not contribute to the terminal voltage, not only remain in the device at short circuit but remain at the same location within the device.

The above numerical result is in agreement with the analytical solution of the continuity equation presented in Equation (4). Comparison of the simulations to the analytical solution is shown in Figure 3, for the illumination wavelength of 750 and 1100 nm, for the same input parameters; excellent agreement observed. Note, a "dead layer" the same thickness as the junction depth (0.4265 μm) was added to the analytical solution of the device at short circuit to account for the absorption in the n-type region that did not contribute to carriers in the bulk p-type region.

In real devices, the above ideal situation can be complicated by an injection dependent lifetime, which alters the sample's recombination properties between open circuit and short circuit conditions and which causes a different voltage independent carrier profile at open circuit and at short circuit conditions, respectively. Furthermore, the above analysis is strictly valid only for a device that is operated in low injection conditions, which justifies the use of the superposition principle.

The impact of the voltage independent carrier density on experimental data is now investigated. For example, the average excess carrier profile under 1100 nm illumination exceeds the voltage dependent carrier profile by 11%. Due to the logarithmic dependence of voltage on carrier density (see detailed discussion below), this deviation represents a moderate overestimation of the implied voltage by 2.7 mV, for this specific case. However, in cases where the operating point of the solar cell is closer to short circuit conditions, as is the case in PL based series resistance imaging, the above percentage increases dramatically (and actually approaches infinity for short circuit conditions), causing much larger errors in implied voltage. The data in Figure 2 show that a suitable approach to reduce these errors is to use short wavelength illumination.

Other experimental methods, which can be strongly affected by voltage independent carriers include the spectral response of photoconductance[13,14] or photoluminescence.[15,16] Figure 4 shows data for the response of photoconductance data[13] and conventional external quantum efficiency data taken on the same sample. Good agreement is observed in the short wavelength range where the voltage independent carriers are negligible. At long wavelength, the voltage dependent carriers increase and result in an over estimation of the external quantum efficiency. For such spectral response measurements, the percentage of the voltage independent carriers to voltage independent carriers directly represents the relative error of the measurement. It is therefore instructive to look at the percentage as a function of illumination wavelengths and for a range of device parameters.

This percentage is, shown in Figure 5, as a function of illumination wavelengths, for a solar cell with the same parameters as above but with varying front surface recombination velocities (S_f). The simulations confirm the above findings; measurements with short wavelength excitation are not at all or only insignificantly affected by voltage independent carriers, whereas measurements at longer wavelength can be severely affected, depending on device parameters. Similar observations were reported earlier,[13–15] but without reference to the fundamental underlying cause. Note that while the above percentage varies strongly with the S_f, the voltage dependent carrier density profile is exactly the same for the different values of S_f. This numerical result is

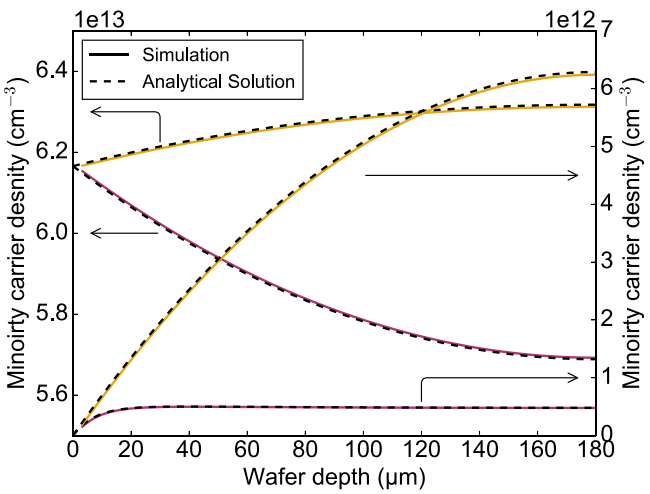

FIG. 3. Comparison of the derived analytical solution with PC1D simulations shown in Figure 2 for the illumination wavelength of 750 and 1100 nm, in the same line styles.

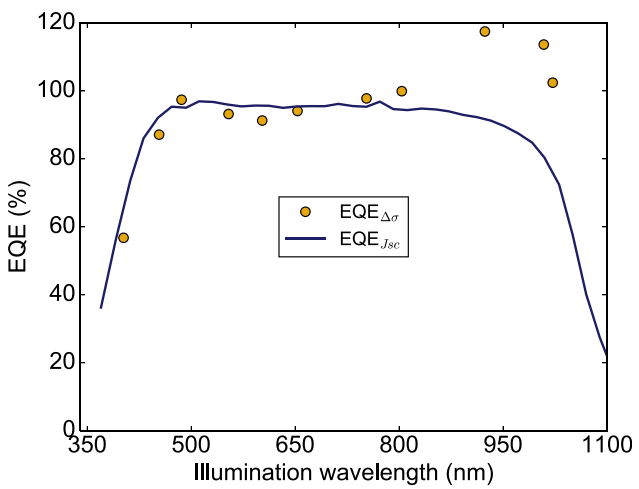

FIG. 4. Comparison of published data for the spectral response of photoconductance with external quantum efficiency measurements taken on the same sample. Data is taken from Ref. 13.

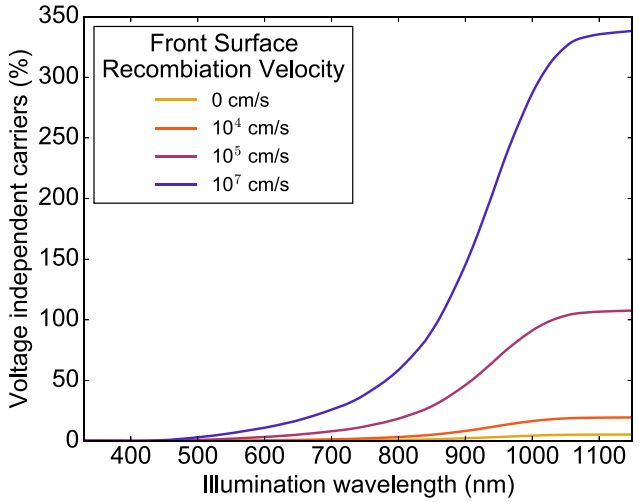

FIG. 5. The percentage of voltage independent carriers to the number of voltage dependent carriers for different front surface recombination velocities.

consistent with the analytical solution and shows that the strong variation in the percentage of voltage independent carriers with S_f shown in Figure 5 is caused entirely by the variation in the voltage dependent carrier density with S_f. This is also true for any recombination within the front diffused region, i.e., voltage independent carriers are not impacted by recombination on the other side of the junction.

Summarising our findings so far, voltage independent carriers affect the implied voltage measurements and spectral response measurements of photoconductance or photoluminescence (both measured under open circuit conditions). The impact voltage independent carriers have is much stronger at long excitation wavelengths and result in error. In spectral response data, these are proportional to the percentage of the voltage independent carrier to the voltage dependent carriers, while errors in implied voltages depend logarithmically on that percentage. In Sec. III, we will analyse how these errors depend on device parameters and provide practical guidelines on parameter combinations, for which voltage independent carriers can be neglected.

III. IMPACT OF VOLTAGE INDEPENDENT CARRIERS

The conditions and device parameter combinations, for which the voltage independent carriers have a negligible impact on the implied voltage will now be analysed for a front junction device.

According to Equations (5)–(7), the voltage independent carriers depend on the samples mobility, bulk diffusion length L, and rear surface recombination velocity S_r. For high bulk lifetimes, and thus large L, the total voltage independent carrier density approaches a limit

$$\lim_{L\to\infty} \overline{n_{vid}} = \lim_{L\to\infty} \int_0^W n_{vid} dx, \tag{12}$$

$$= \frac{N_\gamma}{D\alpha^2}\left(e^{-W\alpha} + W\alpha - 1\right) - \frac{W^2 N_\gamma \left(S_r + e^{-W\alpha}(D\alpha - S_r)\right)}{2\alpha D(D + S_r W)}, \tag{13}$$

which depends only on S_r, the illumination wavelength, and sample thickness. This limit is shown in Figure 6(a) for $W = 0.018\,\text{cm}$, $D = 28.64\,\text{cm}^2\ \text{s}^{-1}$, $N_\gamma = 2.5 \times 10^{17}\,\text{cm}^{-2}\ \text{s}^{-1}$ as a function of S_r for four illumination wavelengths.

The voltage independent carriers decrease with increasing surface recombination for all illumination wavelengths, with longer illumination wavelengths. This is the result of the longer illumination wavelengths generating carriers closer to the rear surface, and hence being more sensitive to the S_r. The saturation at both low and high S_r values is due to the fact that the surface recombination is negligible for well passivated rear surfaces, irrespective of the specific value of

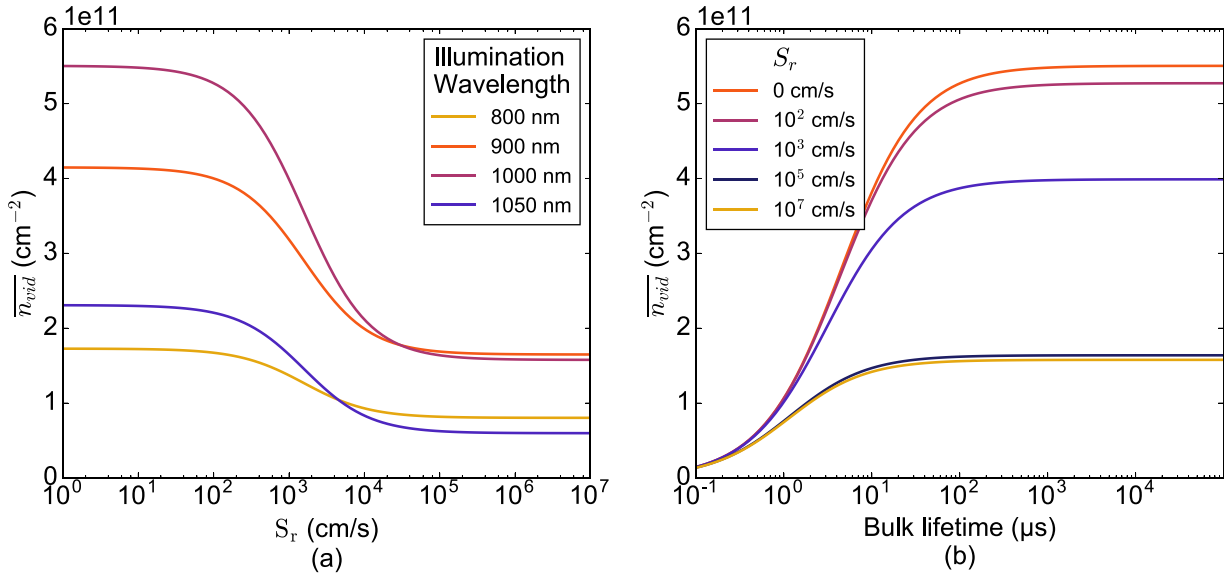

FIG. 6. Average voltage independent carriers density $\overline{n_{vid}}$ calculated with the analytical solution of the continuity equation presented in the text. The average voltage independent carriers density in the high lifetime limit is shown in (a). The impact of bulk lifetime on the average voltage independent carriers is shown in (b) for the illumination wavelength of 1000 nm.

S_r, while for large surface recombination, the rear surface essentially becomes an infinite sink, with the excess carrier density tending towards zero. For values of S_r common in silicon photovoltaic devices ($S_r < 200$ cm/s (Ref. 17)) $\overline{n_{vid}}$ is close to its saturation value. We can thus use this limit as a conservative upper limit that is independent of S_r in the following discussion.

The impact of the bulk lifetime on $\overline{n_{vid}}$ for an illumination wavelength of 1000 nm according to Equation (11) is shown in Figure 6(b). For the simulated 180 μm thick sample, the voltage independent carriers density saturates for bulk lifetimes >200 μs.

A parameter space is now identified for which the deviation between the implied voltage and the junction voltage is <1 mV. Under low injection conditions, the implied voltage ($iVoc$) is calculated from the average excess carrier density as

$$iV_{oc} = V_t \log\left(\frac{\bar{n}N_d}{n_i^2}\right). \tag{14}$$

The junction voltage can be linked to the average voltage dependent carrier density

$$V_{oc} = V_t \log\left(\frac{\overline{n_{vd}}N_d}{n_i^2}\right) + C. \tag{15}$$

The difference between the junction voltage and the implied voltage (ΔV) due to the voltage independent carriers can then be calculated as

$$\Delta V = V_t \log\left(\frac{\bar{n}}{\overline{n_{vd}}}\right). \tag{16}$$

An offset C was added to Equation (15) above, which accounts for the fact that the junction voltage is actually determined by the excess carrier density at the junction, and not the average excess carrier density. For well passivated high lifetime samples, this distinction is irrelevant, since the average carrier density and the carrier density at the junction are very similar and the offset is therefore zero. However, for low diffusion lengths or large surface recombination velocities, the average excess carrier density can be significantly lower than the carrier density at the junction, which the C accounts for. For a constant surface, recombination and diffusion length C is constant and the analysis of the ΔV according to Equation (16) is accurate. If the diffusion length or the surface recombination velocity is injection level dependent, then any analysis of implied voltages is problematic. Correct implied voltage determination then requires a detailed analysis and correction, which are beyond the scope of this paper.

Following on from Equation (16), an implied voltage can thus be considered within 1 mV of the junction voltage if the voltage independent carrier density represents less than 4% of the total excess carrier density. For a given incident photon flux and assuming zero front surface reflection and complete absorption, we find a minimum total excess carrier concentration

$$\Delta n_{min} = N_\gamma A \tau_{eff,min} > \frac{\overline{n_{vid}}}{0.04}, \tag{17}$$

where we define a minimum effective lifetime $\tau_{eff,min}$ for which the voltage independent carriers cause <1 mV absolute error. Using the saturation value for high bulk lifetime and low S_r we can calculate a conservative lower limit for $\tau_{eff,min}$ as a function of wavelength, above which voltage independent carriers do not significantly affect the implied voltage data.

Figure 7 shows $\tau_{eff,min}$ for a 180 μm thick device. As expected from the above discussion, the required effective lifetime is strongly wavelength dependent; a much lower effective lifetime is required at shorter illumination wavelengths. In Sec. II, we defined a minimum lifetime or excess carrier density that is required for the implied voltage to be considered free from the impact of voltage dependent carriers. Alternatively, we can define a minimum required iV_{oc}. The latter is dependent on the sample doping; a sample with higher doping requires a larger minimum iV_{oc}.*

It is interesting to briefly consider the impact of voltage independent carriers on rear junction devices. Clearly, the same deviation between iV_{oc} and V_{oc} must exist for front and rear junction devices for uniform generation rates (illumination wavelengths greater than 1150 nm). However, as the illumination wavelength is decreased, less carriers are collected by a rear junction device, increasing the number of voltage independent carriers, the opposite to a front junction device. Rear junction devices thus require a higher effective lifetime for the impact of the voltage independent carriers to be negligible. It is for this reason that rear junction devices are inherently more sensitive to the impact of voltage independent carriers than front junction devices.

A similar analysis can be carried out for spectral response of photoconductance or photoluminescence data. Here the ratio of the voltage independent carrier density over the voltage dependent carrier density directly represents the relative error. For that error to be <1% the lifetimes shown in Figure 7 must therefore be multiplied by a factor four. It is also noted that the above calculations limiting the value of the effective lifetimes are for measurements taken under open circuit conditions. By the very nature of voltage independent carriers, their relevance on implied

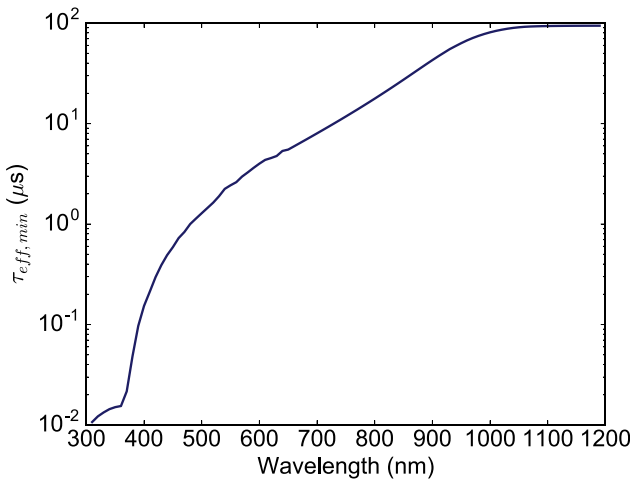

FIG. 7. Minimum effective lifetime for a 180 μm thick sample above which the impact of voltage independent carriers on the implied voltage is <1 mV.

voltages increases tremendously in measurements performed at an operating point below open circuit conditions, since the voltage dependent carrier density is reduced exponentially with voltage, while the voltage independent carrier profile remains the same. As a rule of thumb, the effective lifetime from Figure 7 must be multiplied by a factor of ten for each reduction in junction voltage below V_{oc} by 60 mV. This explains why a correction for voltage independent carrier can still be crucial for samples with effective lifetime far exceeding the limits shown in Figure 7 in experiments in which current is extracted, such as series resistance imaging applications and Suns-PL measurements on shunted samples.

IV. CONCLUSION

This paper set out the terminology for voltage dependent and voltage independent carriers and described how they impact implied voltage measurements and the spectral response of photoconductance and photoluminescence. Voltage independent carrier density profiles in silicon solar cells were calculated determined analytically using solutions to the continuity equation for the quasi neutral region. The calculations showed that the same voltage independent carrier density profile remains in the bulk at operating points between open circuit conditions and short circuit conditions, which retrospectively provides the basis for correction methods previously applied to photoluminescence based characterisation methods such as Suns-PL and PL based series resistance imaging.

It was shown that the presence of voltage dependent carriers depends strongly on device parameters and on the illumination wavelength, showing that the impact of voltage independent carriers is much lower for short illumination wavelengths. Absolute errors in implied voltages depend logarithmically on the ratio of average voltage independent carriers to voltage dependent carriers, whereas errors in spectral response measurements are dependent linearly on that ratio. Practical limits for when a sample is virtually free from the impact of the voltage independent carriers were determined.

ACKNOWLEDGMENTS

The Australian Centre for Advanced Photovoltaics is supported by the Australian Government through the Australian Renewable Energy Agency (ARENA). The Australian Government does not accept responsibility for the views, information, or advice expressed herein.

[1]M. Wolf and H. Rauschenbach, Adv. Energy Convers. **3**, 455 (1963).
[2]R. A. Sinton and A. Cuevas, in *16th European Photovoltaic Solar Energy Conference* (Glasgow, 2000), pp. 1152–1155.
[3]R. A. Sinton and A. A. Cuevas, Appl. Phys. Lett. **69**, 2510 (1996).
[4]T. Trupke, R. A. Bardos, M. D. Abbott, and J. E. Cotter, Appl. Phys. Lett. **87**, 093503 (2005).
[5]T. Trupke, E. Pink, R. A. Bardos, and M. D. Abbott, Appl. Phys. Lett. **90**, 093506 (2007).
[6]M. D. Abbott, R. A. Bardos, T. Trupke, K. C. Fisher, and E. Pink, J. Appl. Phys. **102**, 044502 (2007).
[7]D. Clugston and P. A. Basore, in 26th Photovoltaic Specialists Conference (IEEE, Anaheim, 1997).
[8]M. Glatthaar, J. Haunschild, R. Zeidler, M. Demant, J. Greulich, B. Michl, W. Warta, S. Rein, and R. Preu, J. Appl. Phys. **108**, 014501 (2010).
[9]U. Rau, IEEE J. Photovoltaics **2**, 169 (2012).
[10]D. Lan and M. A. Green, Sol. Energy Mater. Sol. Cells **134**, 346 (2015).
[11]W. Shockley and W. Read, Phys. Rev. **87**, 835 (1952).
[12]R. Hall, Phys. Rev. **87**, 387 (1952).
[13]H. Mäckel and A. Cuevas, in International Solar Energy Society Solar World Congress (Adelaide, 2001).
[14]A. Cuevas, R. A. Sinton, M. J. Kerr, D. MacDonald, and H. Mäckel, Sol. Energy Mater. Sol. Cells **71**, 295 (2002).
[15]D. Berdebes, J. Bhosale, K. H. Montgomery, X. Wang, A. K. Ramdas, J. M. Woodall, and M. S. Lundstrom, IEEE J. Photovoltaics **3**, 1342 (2013).
[16]M. K. Juhl, M. D. Abbott, Y. Li, Z. Li, D. Lin, N. Borojevic, and T. Trupke, in *29th European Photovoltaic Solar Energy Conference* (Amsterdam, 2014), pp. 455–458.
[17]A. Fell, K. R. McIntosh, P. P. Altermatt, G. J. M. Janssen, R. Stangl, A. Ho-Baillie, H. Steinkemper, J. Greulich, M. Muller, B. Min, K. C. Fong, M. Hermle, I. G. Romijn, and M. D. Abbott, IEEE J. Photovoltaics **1**, 1250–1263 (2015).